Electronic Supplementary Material (ESI) for New Journal of Chemistry.
This journal is © The Royal Society of Chemistry and the Centre National de la Recherche Scientifique 2018

Electronic Supplementary Information (ESI)

Boronate–decorated porous carbon material derived from zinc-based metal–organic framework for enrichment of cis–diol–containing nucleosides

Yanan Pan[†], Xiumei Guo[†], Shanshan Li[†], Xiaoyan Liu[†*], Haixia Zhang[†]

[†] State Key Laboratory of Applied Organic Chemistry, Key Laboratory of Nonferrous Metals Chemistry and Resources Utilization of Gansu Province and College of Chemistry and Chemical Engineering, Lanzhou University, Lanzhou 730000, China.

Table of Contents

[*] Corresponding author Tel: +86-931-8912510; fax: +86-931-8912582;
E-mail: liuxiaoy@lzu.edu.cn

Section 1. Synthesis of zinc-based metal–organic framework

The ligand 2,5-bis (phenylamino)-1,4-benzenedicarboxylic acid (L) was synthesis according to the literature procedure with minor modification.[1] The zinc-based metal–organic framework (Zn–MOF) was prepared under solvothermal condition. The details of procedure are described as follows:

A mixture of $Zn(NO_3)_2 \cdot 6H_2O$ (0.10 mmol), L (0.10 mmol), and DMF:H_2O (4.0 mL, v/v = 8:1) was sealed in a pressure-resistant glass tube, and then heated to 75 °C for 48 h. Subsequently, the contents were cooled down to room temperature, which afforded orange crystals in 50% yield (based on L).

Section 2. Characterization

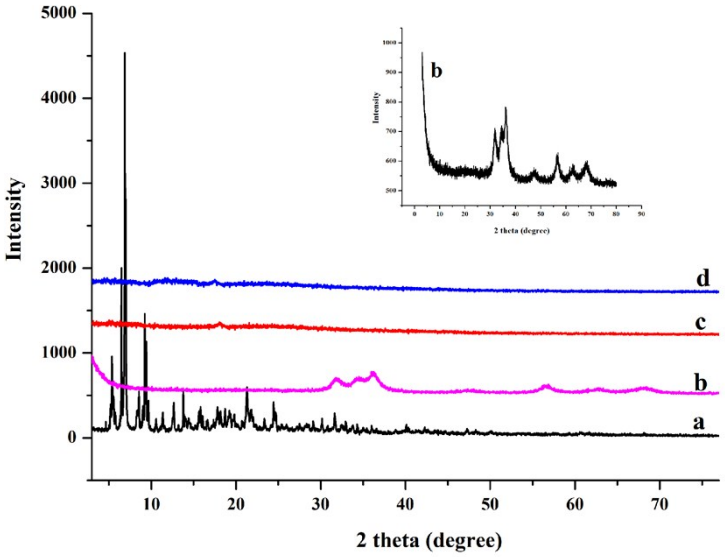

Fig. S1 PXRD patterns of (a) the parent Zn–MOF, (b) C_{MOF}, (c) C_{MOF}–COOH, and (d) boronate–decorated C_{MOF}.

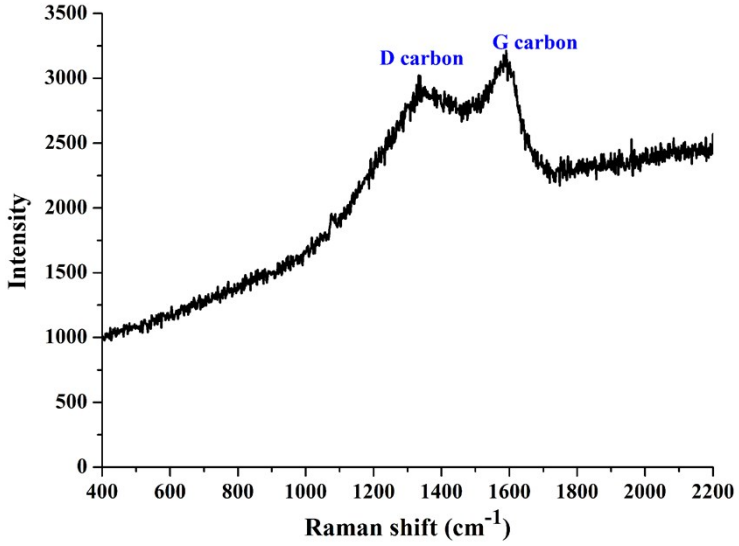

Fig. S2 The Raman spectrum of boronate–decorated C_{MOF}.

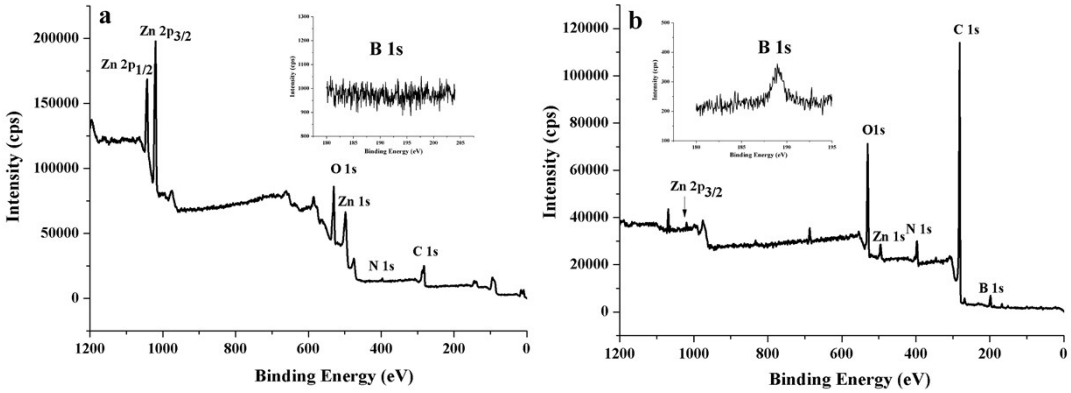

Fig. S3 XPS spectra of (a) C_{MOF}, and (b) boronate–decorated C_{MOF}.

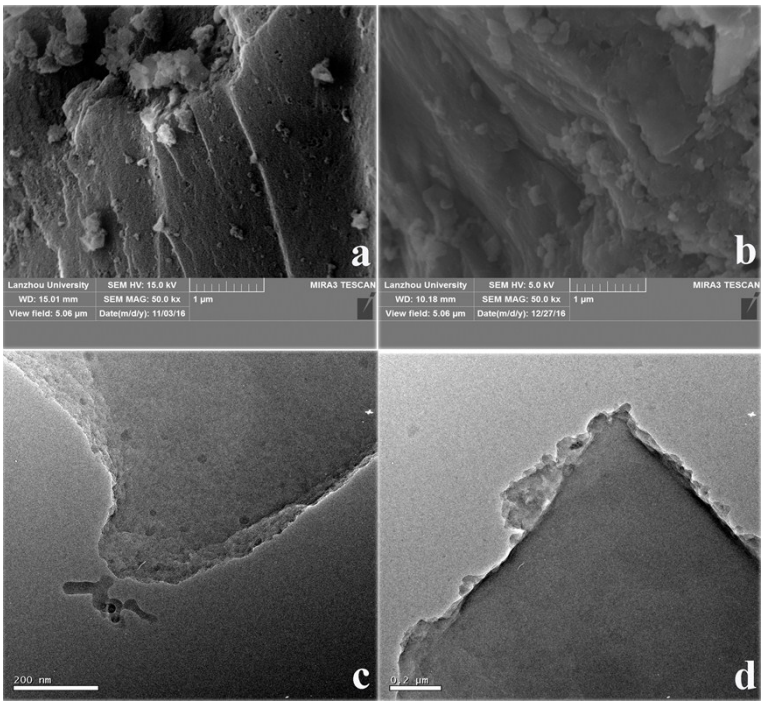

Fig. S4 SEM (a, b) and TEM (c, d) images of C_{MOF} (a, c) and boronate–decorated C_{MOF} (b, d).

Table S1 Physicochemical properties of Zn-MOF, C_{MOF} and boronate–decorated C_{MOF}.

	S_{BET} / (m^2 g^{-1})[a]	V_{BJH} / (cm^3 g^{-1})[b]		D_{BJH} / (nm)[c]	
		Adsorption	Desorption	Adsorption	Desorption
Zn-MOF	1.64	0.0013	0.0014	9.19	52.2
C_{MOF}	0.15	/[d]	/[d]	/[d]	/[d]
boronate–decorated C_{MOF}	37.2	0.018	0.016	4.10	3.26

[a] BET surface area.

[b] BJH adsorption and desorption cumulative volume of pores.

[c] BJH adsorption and desorption average pore width (4V/A).

[d] These data cannot be detected by instrument.

Section 3. Optimization of the extraction and desorption conditions

Optimization of desorption time and desorption times

It is well known that the boronate affinity mechanism relies on pH–controlled capture or release.[2] Herein, we choose 5% TFA–methanol as the desorption solvent. Fig. S5 shows that 3.0 min of desorption time and twice elution processes can complete the desorption of all analytes.

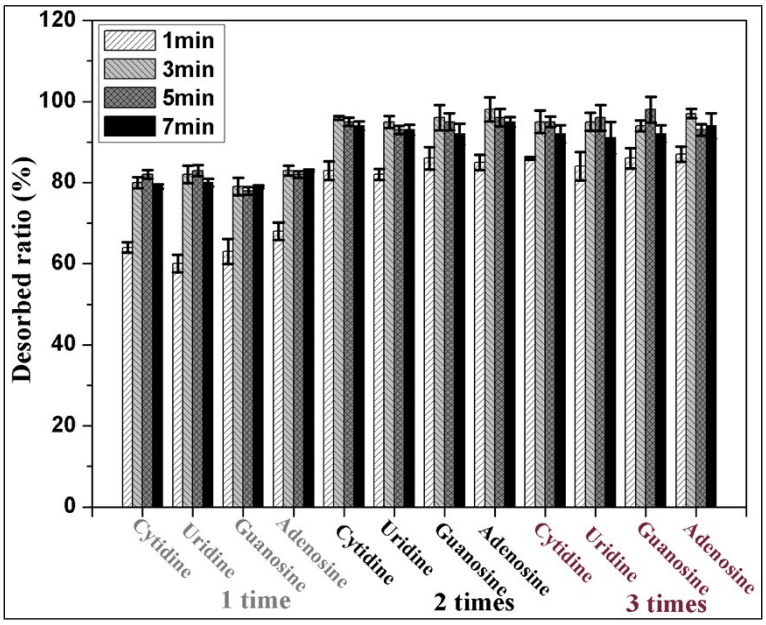

Fig. S5 Effect of desorption time and desorption times on extraction of nucleosides. Date are mean ± standard deviation (SD, n=3). Extraction conditions: sample volume: 2.0 mL; samples solution: 2.0 μg mL^{-1} for cytidine, uridine, guanosine and adenosine; desorption solvent: trifluoroacetic acid: methanol = 5:95 (v/v); desorption solvent volume: 0.4 mL.

Optimization of extraction conditions

The extraction conditions such as extraction time, extraction pH, ionic strength, and the amount of adsorbent were optimized separately. Fig. S6a shows that all analytes reach the extraction equilibrium in 25 min. At the same time, consistent with

the boronate affinity mechanism, the experimental results (Fig. S6b) establish that the extraction should be implemented under alkaline condition and pH of 9.0 was selected. Furthermore, the effect of salt addition was investigated by changing NaCl concentration. Fig. S6c shows that the extraction efficiency declined with the increased content of NaCl in sample solutions. In general, the presence of NaCl will reduce the solubility of analytes in water, which would increase the hydrophobic interaction between analytes and adsorbent. However, the boronate affinity materials usually show excellent water dispersibility and provide specific affinity interaction towards hydrophilic cis–diol compounds.[3] Therefore, the addition of salt cannot improve the extraction efficiency for hydrophilic nucleosides and sample matrix without addition of NaCl was selected for further investigation. Finally, the different amounts (3.0, 5.0, 7.0 and 9.0 mg) of adsorbent was used to test the extraction efficiency. Fig. S6d finds that the extraction efficiencies increase with the increased amount of adsorbent, then tend to be unchanged. Considering that the concentration of nucleosides in biological samples is usually lower than 2.0 μg mL^{-1}, 7.0 mg of adsorbent was applied in the following analysis of nucleosides in real samples.

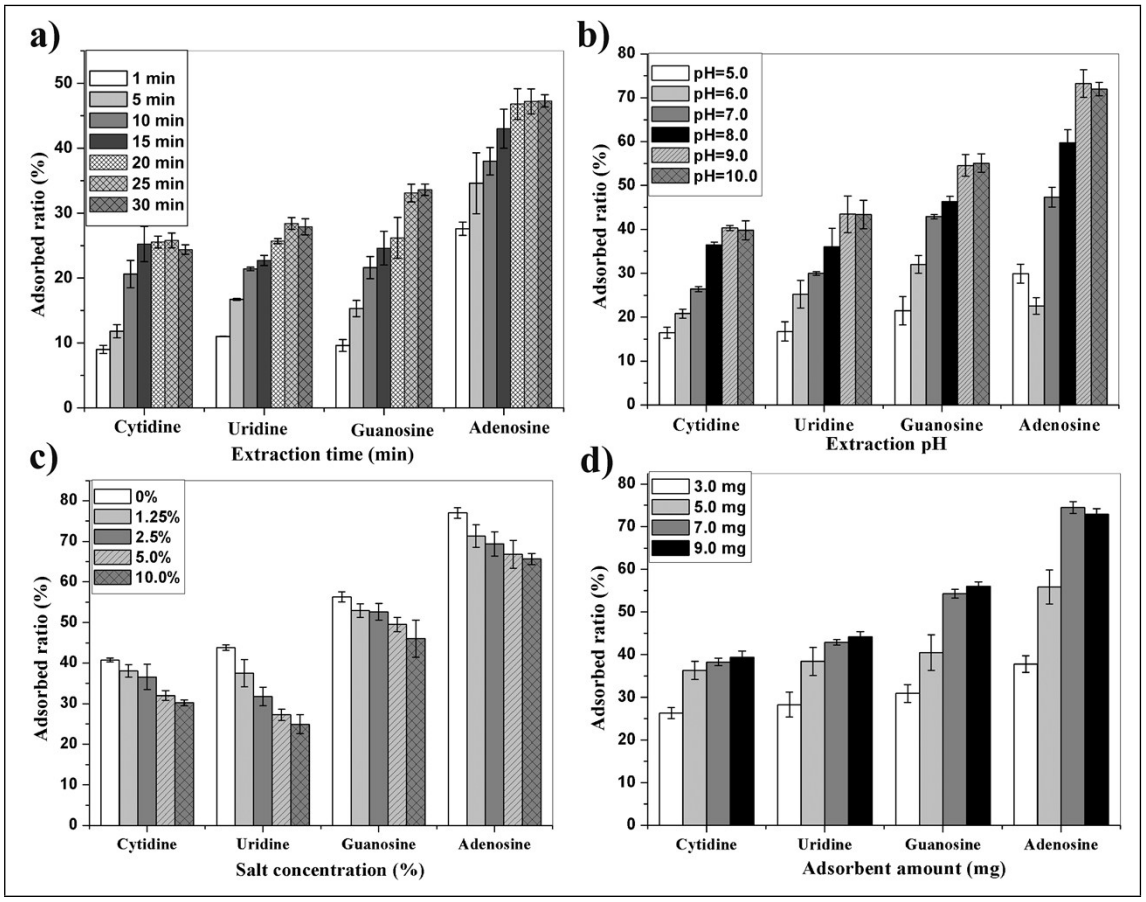

Fig. S6 Effect of extraction conditions on extraction of nucleosides. Data are mean ± SD (n=3). Sample volume: 2.0 mL; samples solution: 2.0 μg mL^{-1} for cytidine, uridine, guanosine and adenosine; desorption solvent: trifluoroacetic acid: methanol = 5:95 (v/v); desorption solvent volume: 0.4 mL.

Section 4: Adsorption capacity and selectivity

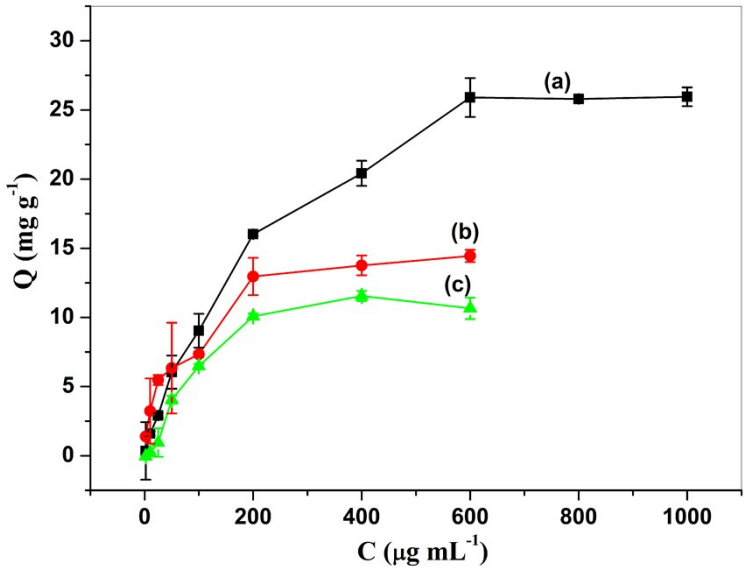

Fig. S7 Adsorption capacity of (a) boronate–decorated C_{MOF}, (b) C_{MOF} and (c) calcined ligand toward adenosine.

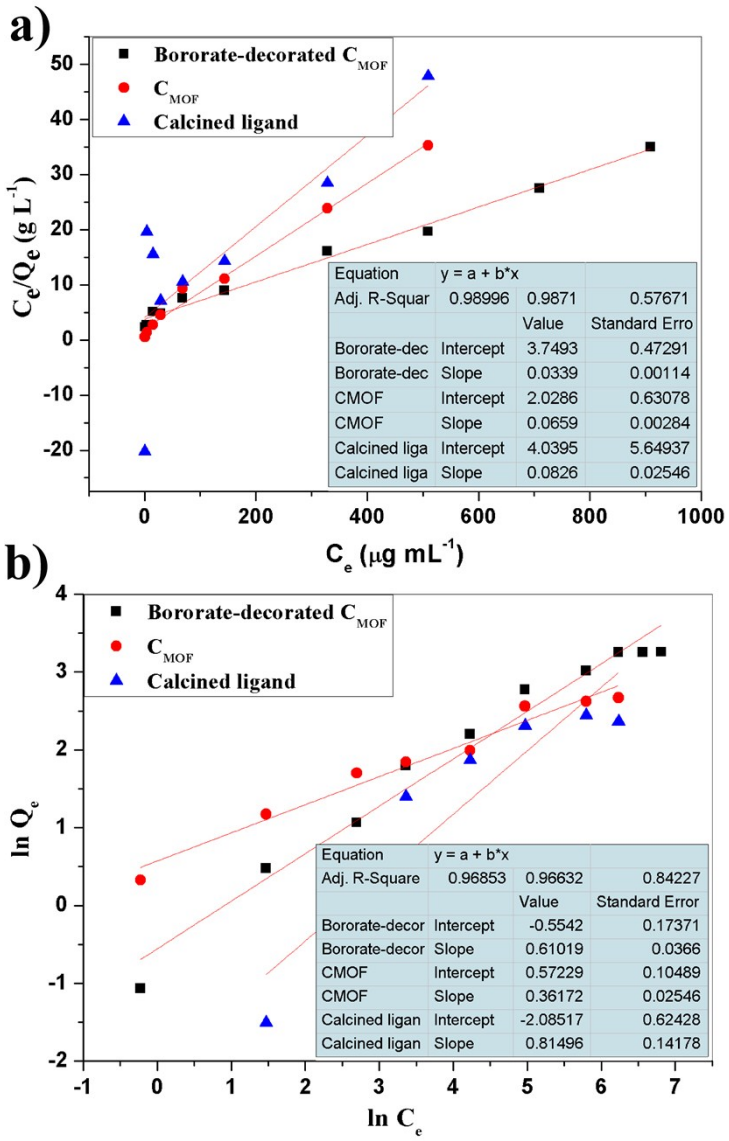

Fig. S8 Langmuir (a) and Freundlich (b) plot of different adsorbents for adsorption of adenosine.

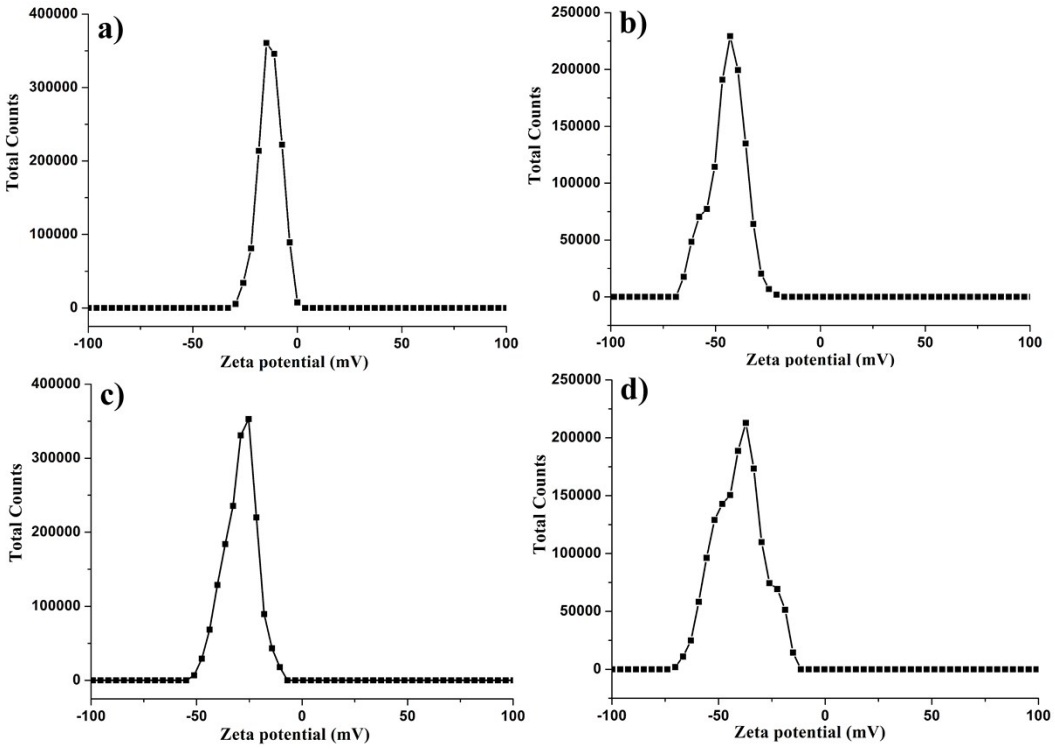

Fig. S9 Zeta potential distribution of the C_{MOF} before (a) and after (b) adsorption of adenosine, and boronate–decorated C_{MOF} before (c) and after (d) adsorption of adenosine.

Table S2 Adenosine adsorption parameters for Langmuir and Freundlich models.

Adsorbents	Langmuir $\frac{Ce}{Qe} = \frac{1}{KLQm} + \frac{Ce}{Qm}$			Freundlich $\ln Q_e = \ln K_f + \frac{1}{n} \ln C_e$		
	Q_m (mg g^{-1})	K_L (L mg^{-1})	R^2	K_f (L mg^{-1})	n	R^2
Boronate–decorated C_{MOF}	29.4	0.0091	0.9900	0.575	1.639	0.9685
C_{MOF}	15.2	0.0325	0.9871	1.772	2.765	0.9663
Calcined ligand	12.1	0.0205	0.5767	0.124	1.227	0.8423

where C_e is the equilibrium concentration of adenosine; Q_e is the equilibrium adsorption capacity; Q_m is the maximum monolayer coverage capacity; K_L is the Langmuir isotherm constant; K_F is the Freundlich isotherm constant; n is the adsorption intensity.

Section 5: Evaluation of Method

Table S3 Analytical performances of the developed methods.

Compounds	Linear range (μg L^{-1})	Calibration curves	R^2	LOD (μg L^{-1})	LOQ (μg L^{-1})
Cytidine	50–2000	y=0.167x-0.0744	0.9975	14.6	50
Uridine	50–2000	y=0.177x-0.0744	0.9980	13.8	50
Guanosine	25–2000	y=0.335x-1.0740	0.9961	7.29	25
Adenosine	25–2000	y=0.516x+6.9233	0.9980	4.73	25

Table S4 Recoveries and precisions of the four nucleosides in three practical samples obtained by the developed method.

Samples	Compounds	Spiked（μg L^{-1}）	Found (μg L^{-1})	Recovery (%)	RSD[b] (%)
Injection sample	Cytidine	0.0	52.10		5.2
		50.0	100.0	95.8	3.9
		100.0	153.4	101.3	4.9
		500.0	563.6	102.3	7.3
	Uridine	0.0	ND[a]		/
		50.0	48.10	96.2	7.8
		100.0	95.3	95.3	9.8
		500.0	506.5	101.3	8.7
	Guanosine	0.0	445.0		6.4
		50.0	491.0	92.0	7.2
		100.0	540.0	94.6	2.2
		500.0	917.0	94.5	9.6
	Adenosine	0.0	45.90		6.1
		50.0	94.6	97.4	10.1
		100.0	142.2	96.3	8.3
		500.0	513.7	93.6	4.8
$HepG_2$ cell	Cytidine	0.0	44.10		7.7
		50.0	88.2	88.2	3.6
		100.0	142.4	98.3	4.7
		500.0	527.0	96.9	8.6
	Uridine	0.0	53.20		7.5
		50.0	99.2	92.0	6.4
		100.0	144.5	91.3	7.4
		500.0	574.6	104.3	9.9
	Guanosine	0.0	429.0		6.4
		50.0	476.0	94.0	2.6
		100.0	519.7	90.7	5.3
		500.0	905.0	95.2	9.4
	Adenosine	0.0	586.0		5.4
		50.0	633.0	94.0	2.7
		100.0	688.3	102.3	6.8
		500.0	107.0	97.6	5.9
F_9 cell	Cytidine	0.0	ND		/
		50.0	47.40	94.8	2.5
		100.0	95.3	95.3	7.6
		500.0	469.6	93.9	6.9
	Uridine	0.0	58.60		3.2
		50.0	112.0	106.8	10.2
		100.0	151.9	93.3	7.4

	500.0	502.1	88.7	3.8
Guanosine	0.0	539.0		2.5
	50.0	584.0	90.0	7.9
	100.0	631.5	92.5	11.3
	500.0	992.9	90.8	5.4
Adenosine	0.0	529.0		7.3
	50.0	576.0	94.0	8.5
	100.0	618.3	89.3	1.3
	500.0	965.6	87.3	9.7

[a] ND: Not detected.

[b] RSD: Relative standard deviation

Section 6. References

1 J. Shi, S. Zheng, *Macromolecules.,* 2001, **34**, 6571.

2 L. Gao, C. Wang, Y. Wei, *Rsc Adv.,* 2016, **6**, 28470.

3 H. Li, H. Wang, Y. Liu, Z. Liu, *Chem Commun.,* 2012, **48**, 4115.